

Study of diffusion processes in contact areas of thermocouples with metals

K. Onarkulov¹ and T. Azimov^{1*}

¹Fergana State University, 19, Murabbiya Str., 150100, Fergana city, Uzbekistan

Abstract. Diffusion processes on the contact areas of the metal-solder-semiconductor system are experimentally studied in this work. Diffusion coefficients, activation energies and pre-exponential factors in samples commutated with solders based on Pb-Sb are determined. It has been established that lead-based solder has a significantly higher inertness to thermoelectric materials. Key words: diffusion, alloy, thermoelement, solder, contact, thermopile, activation energy, chemical activity. Humans are currently facing complex challenges such as rising energy costs, pollution and global warming. To reduce their consequences, scientists are concentrating on improving power generators focused on energy harvesting. Thermoelectric generators (TEGs) have demonstrated their ability to convert thermal energy directly into electricity through the Seebeck effect. Due to the unique advantages, they present, thermoelectric systems have emerged over the past decade as a promising alternative among other technologies for the production of clean energy. [1-11]. Switching is the most time-consuming and responsible operation in the manufacture of thermoelectric modules. In them, which include a significant number of junctions, failures most often occur due to broken contacts [2-8]. To prevent the harmful effects of internal mechanical stresses, in the manufacture of thermoelectric batteries, it is necessary to use a damping layer between the branch and the connecting plate [3-14]. The damping layer is made of a material with sufficient plasticity and low ohmic resistance. It is usually made from lead. The results of the research showed the advantages of using a single -wire technology for soldering with Pb - Sb eutectic solder using an anti -diffusion layer of chemically deposited nickel. In this case, the eutectic solder Pb - Sb in the contact simultaneously performs the role of a damper and a switching solder.

1 Introduction

1.1 Technology for manufacturing prototypes of thermopiles

For experimental verification of the properties of the developed thermoelectric materials and switching technology, prototypes of thermoelectric modules were made, consisting of 24 and 95 thermoelements. Thermoelement legs were made of zone -directed crystals $\text{Bi}_2\text{Te}_{2.88}\text{Se}_{0.12}$

*Corresponding author: tmazimov@mail.ru

+0.04 wt. % Ni +0.05 wt. % Sb with Q factor $2.7 \cdot 10^{-3} \text{ K}^{-1}$ and $\text{Sb}_{1.5}\text{Bi}_{0.5}\text{Te}_3$ +3 wt. % Te +0.05 wt. % Ni with a quality factor of $3 \cdot 10^{-3} \text{ K}^{-1}$.

Of thermoelement legs were cut from an ingot of thermoelectric material by the electro spark method, and the height of the billets was equal to the height of the finished legs. Branch blanks were etched twice in a 50% nitric acid solution for 15 seconds. After etching, the workpieces were boiled in ethanol and dried in air. The ends of the thermoelement legs were chemically coated with a nickel-phosphorus film using a solution of the composition $\text{NiCl} \cdot 6\text{H}_2\text{O} - 30\text{g/l}$, $\text{NH}_4\text{Cl} - 30\text{g/l}$ with the addition of sodium citric acid up to 45 gr/l. The alkalinity (pH) of the resulting solution was brought to a value of 10 - 10.5 with ammonia, and sodium hypophosphate was added to the solution in an amount of 15 gr / l.

2 Experimental technique

The process of applying the nickel-phosphorus coating was carried out at a temperature of $85 \div 87 \text{ }^\circ\text{C}$ in the presence of a nickel plate for 4 minutes. After coating, the workpieces were washed in running and distilled water, wiped with alcohol, and annealed at a temperature of $225 \pm 3 \text{ }^\circ\text{C}$ for 2 hours.

Copper busbars were coated with a nickel-phosphorus coating according to the method described in [4-6]. Blanks of thermoelement legs and busbars were tinned with Pb - Sb eutectic solder. After tinning, branches of thermocouples sized $2 \times 2 \times 4$ were cut by the method of electric spark cutting mm and $3 \times 3 \times 4$ mm and soldered together with current-carrying tires. Soldering was carried out at a temperature of $280 \pm 3 \text{ }^\circ\text{C}$. On fig. one shows the layout of the elements of a single thermoelement.

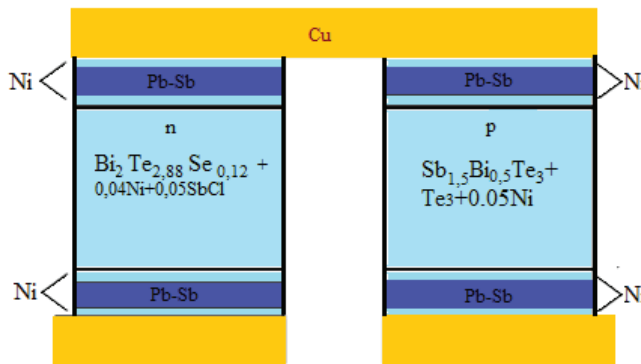


Fig. 1. Scheme of arrangement of elements of a single thermoelement.

The quality control of thermopile switching was carried out by external inspection. The magnitude of the voltage drop was tested on one thermoelement at the optimum current. The control was carried out by placing a millivoltmeter probe in turn on each subsequent thermoelement in the direction of the switching stroke. The value of the voltage drops on individual branches or thermoelements of the thermoelectric battery did not differ by more than $\pm 3\%$. Voltage drops exceeding the specified limit indicate their poor-quality switching. A significant increase in the voltage drop across the thermoelement corresponds to a switching failure as a result of thermal stresses or mechanical damage, and a decrease in the voltage drop from the norm corresponds to the presence of a short circuit in the battery, which most often occurs due to the influx of solder on the semiconductor.

Proposed The technology greatly simplifies the process of assembling thermopiles, increases their efficiency, and also makes it possible to mechanize the process of applying solder to a thermoelement, which is very important in serial production of thermoelectric batteries. In addition, it allows to significantly expand, for example, up to $450 \text{ }^\circ\text{K}$, the

temperature of the environment in which the thermopile functions normally.

3 Thermoelectric modules

An experimental verification of the previously obtained results was carried out on individual half-elements, with the manufacture and testing of cooling thermopile at elevated temperatures. The external view of the experimental module, consisting of 24 thermoelements with a total working surface of 875 mm², is shown in Fig. 2.

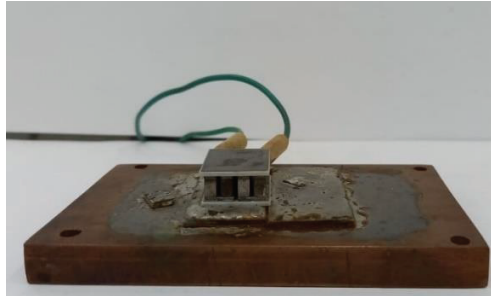


Fig. 2. Appearance of the experimental module, consisting of 24 thermocouples with a total working surface of 875 mm².

Tests of prototype thermopile samples to achieve the maximum temperature difference were carried out in a vacuum of the order of 10⁻³ Pa with an increase in the temperature of the hot junction from 320 to 495 K. Cooling was carried out with running water, the heat load to the cold junction of the thermopile came from an electric heater. The temperature at the junctions was controlled by chromel-alumel thermocouples ($\varnothing = 0.3$ and 0.5 mm) in an electrically insulating braid, directly behind thermopile bars minted into electrically conductive tires on the hot side and metal plates on the cold side.

4 Experimental results

The maximum temperature difference ΔT_{\max} for is one of the main characteristics of a cooling thermopile. The real efficiency (Z) of a thermopile is quite simply and reliably determined from the maximum temperature difference it develops. This way of determining Z is reduced to measuring T and $T_{0\min}$ at the junctions of the thermopile under conditions of its adiabatic isolation. But in our case, the testing of cooling thermopile at elevated temperatures artificially creates thermal loads to the cold junction, as a result of which the efficiency of the module is underestimated.

The dependence of the thermoelectric efficiency of the module on the temperature of the hot and cold junctions in the operating mode is presented in Table 1.

Table 1. The dependence of the thermoelectric efficiency of the module on the temperature of the hot and cold junctions in the operating mode.

I_{\max}, A	$(T_1), K$	ΔT	$(T_2), K$	$Z \cdot 10^{-3} K^{-1}$
4.9	320	35	285	0.86
5.0	370	50	320	0.98
5.1	470	60	360	0.93
5.2	480	68	402	0.84
5.2	495	70	425	0.76

As can be seen from Table 1, the thermopile power supply parameter was maintained

with an accuracy of ~6%.

The results of measurements of ΔT under conditions of adiabatic insulation (1) and in a thermal load of 3 W to the cold junction (2) are shown in Fig.3. It can be seen from Fig. 3 that the thermal load to the cold junction leads to a significant decrease in ΔT (up to 40), while the resistance of the thermopile increased from 0.48 Ohm to 69 Ohm. However, it should be noted that a rather significant decrease in ΔT_{\max} and an increase in resistance to a cold junction under thermal load can be explained not only by the influence of contact resistances, but also by the specific conditions for the technological process of manufacturing prototypes.

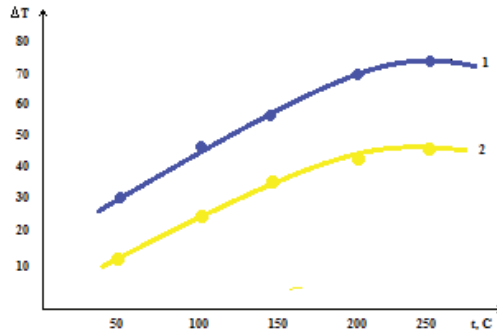


Fig. 3. Dependence of the temperature difference (ΔT) on the ambient temperature (T_c). 1 - no load 2 - load 3 watts.

At a zero-temperature gradient ($\Delta T=0$) in the thermopile, the maximum cooling capacity Q was determined. An increase in T_x from $T_{x\min}$ to $T_x = T_h$, the resistance of the thermopile was equal to $R=0.74$ Ohm and the value of the maximum cooling capacity calculated at this $Q = 6.24$ W.

An analysis of the experimental data shows that the thermopile of solder-bonded Pb-Sb eutectics with an anti-diffusion nickel layer can be effectively used for temperature control or cooling of various objects in the temperature range (200÷473) K.

5 Determination of contact resistance

When measuring the maximum temperature difference ΔT_{\max} of thermoelements, as a rule, the optimal operating current I_{opt} and the maximum voltage drop U_{\max} are also measured. In this case, without additional measurements, it is possible to determine one of the factors influencing the efficiency of a thermoelement - the contact resistance r_c .

The essence of the method is that at a value of $(\Delta T)_{\max}=0$, based on a fixed I_{\max} and U_{\max} , contact resistances are determined.

It is known that in the mode of maximum cooling capacity in the absence of external heat load, the optimal thermoelement current is determined [10-18] by the formula

$$I_{\text{opt}} = \frac{\alpha T_x}{R+2r_c} \quad (1)$$

from here

$$r_c = \frac{\alpha T_x - IR}{2I} = \frac{\alpha T_h - \alpha \Delta T - IR}{2I} \quad (2)$$

Considering that $\Delta T = 0$ then

$$r_c = \frac{\alpha T_h - IR}{2I} = \frac{U - I\rho \frac{2l}{S}}{2I} \quad (3)$$

Here, the influence of two contact resistances between the branches and the connecting plate is taken into account. Taking into account two more contact resistances on the hot sides of the thermoelement legs, we can write

$$r_c = \frac{U - I\rho \frac{2l}{S}}{2I} \quad (4)$$

where U is the voltage drop across the ohmic resistance of the thermoelement branch, V;

S- cross-sectional area (cm²), l- height of thermoelement leg (cm);

ρ - electrical resistivity of the material, Ω cm.

Thus, (4) makes it possible to calculate the value of the contact resistance indirectly, based on measurements of the voltage drop across the thermoelement, at the optimum value of the operating current I_{opt} and $\Delta T = 0$ ($\Delta T = T_h - T_x$), those. at $T_h = T_x$.

Table 2 shows the contact resistance values determined by this method and for comparison, the values of r_c measured by probe methods are given.

Table 2. Comparative evaluation of contact resistance depending on the parameter of thermoelements.

N_2	I_{opt} A	U_{max} V	l sm	S sm ²	r_c $\Omega \cdot \text{sm}^2$	r_c $\Omega \cdot \text{sm}^2$ (probe method)
1	74	0.0912	0.3	0.5	$0.4 \cdot 10^{-5}$	$1.6 \cdot 10^{-5}$
2	23	0.096	0.3	0.4	$1.08 \cdot 10^{-5}$	$1.9 \cdot 10^{-5}$
3	13	0.102	0.3	0.3	$0.19 \cdot 10^{-5}$	$1.02 \cdot 10^{-5}$
4	6	0.100	0.3	0.2	$1.06 \cdot 10^{-5}$	$2.1 \cdot 10^{-5}$
5	1.6	0.102	0.3	0.1	$1.9 \cdot 10^{-5}$	$2.09 \cdot 10^{-5}$

Temperature is one of the main factors affecting the structure, i.e., on the intramolecular relationship in the volume of the solder layer. Therefore, any change in this layer, for example, the appearance of microcracks, solder loosening, delamination of the nickel film from the working surface of the branch, will lead to a change in the resistance of the layer. Therefore, it is very important to establish the effect of temperature cycling alternating cold - heat on the resistance of the solder layer. If the narrowing and expansion of the volume of the interlayer with a change in the temperature of the latter will be within acceptable limits, then the resistance of the interlayer will not change. In order to determine the effect of temperature cycling, the following study was carried out. After the thermoelement enters the mode, i.e., when the temperature at the cold junction reached the minimum value T_{min} , by changing the direction of the current, the cold junction was heated up to 100°C. Then, switching to the cooling mode, the cold side was again reached T_{min} within 20 minutes. After each repetition of the specified cycle 10 times, the contact resistance was measured according to the method described above. The obtained results of the dependence of r_c on the temperature shock number n are shown in Fig. 4.

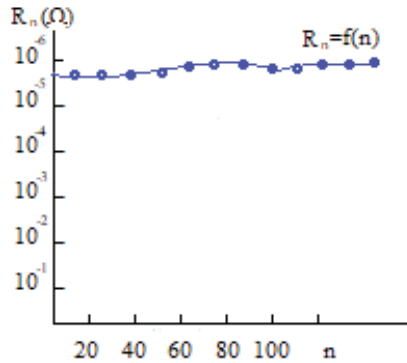


Fig. 4. Dependence of the contact resistance on the number of switching of the operating mode of the thermoelement.

Measurements show that the contact resistance does not exceed $\sim 1.2 \cdot 10^5 \Omega \cdot \text{cm}^2$, which fully satisfies the requirements for high-quality switching of thermopile.

Thus, the proposed method for determining the contact resistance of contacts is a simple and affordable method and does not require acutely scarce highly sensitive measuring instruments. This technique allows us to investigate the influence of various factors on the value of the switching resistance.

6 Conclusion

1. Pb-Sb found that the activation energy Diffusion of the solder is greater (52500 J/mol) in the case of switching contacts with eutectic alloy Pb-Sb than switching solder Bi-Sb • This indicates that the eutectic alloy Pb-Sb is a promising switching material for cooling thermopiles operating at elevated temperatures as well as for thermocouples operating in vacuum.
2. As a result of the study of the physico-chemical compatibility of the eutectic alloy of the Pb-Sb system with $\text{Bi}_2 \text{Te}_{2.88} \text{Se}_{0.12}$ and $\text{Bi}_{0.5} (\text{Sb})_{1.5} (\text{Te})_3$ solid solutions, the possibility of using this alloy, which has a melting point of 525 K. as a solder for single-layer switching of thermopiles operating in the temperature range (200 ÷ 450) K in vacuum.
3. It has been established that chemical deposition of nickel on contact surfaces excludes reactive diffusion of solder components up to 473 K and provides good wettability of both Bi-Sb and Pb-Sb solders.
4. An installation for controlling the mechanical strength in compression of semiconductor materials has been developed and manufactured. Tests were carried out under conditions of repeated thermal cycling.

References

1. A.S. Oxotin, *Sostoyaniye i perspektivy termoelektricheskogo preobrazovaniya teplovooy energii v elektricheskuyu* (Izvestiya Moskovskogo gosudarstvennogo industrialnogo universiteta, Moskva, 2008)
2. G. Sun, X. Qin, D. Li, J. Zhang et al, *Alloys Compd* **639**, 9–14 (2015)
3. E.M. Lukisher, A.L. Vayner, M.N. Somkin, V.Yu, *Vodolagin Termoelektricheskie oxladiteli* (Radio i svyaz, M., 1983)
4. M. Xansen, K. Anderko, *Struktury dvoynyx splavov t. I, II* (Metallurgizdat, M., 1962)

5. K.E. Onarkulov, A.A. Yuldashev, T. Azimov, Sh. Yo'ldoshqori, FarDU ilmiy xabarlar **2**, 32-35 (2017)
6. K. Onarkulov, Y. Usmanov, T. Azimov, European Journal of Molecular & Clinical Medicine **7.2**, 2353-2358 (2020)
7. K. Onarkulov, Y. Usmanov, T. Azimov, Austrian Journal of Technical and Natural Sciences **1-2**, 16-20 (2020)
8. A.V. Karimov et al., Technology and design in electronic equipment -Odessa **4**, 23-28 (2007)
9. T. Azimov et al., American Journal of Modern Physics **10.6**, 124-128 (2021)
10. Bozorovich, Nabiev Makhmud, et al., Problems of modern science and education **12-2(145)**, 69-73 (2019)
11. K.E. Onarkulov, T.M. Azimov, M.K. Onarkulov, Yangi materiallar va geliotexnologiyalar **46** (2020)
12. K. Daliev, T. Azimov, M.Onarkulov, Euroasian Journal of Semiconductors Science and Engineering **2.1**, 1 (2020)
13. A.V. Dmitriev, Uspehi fiz. Nauk **180(8)**, 821–837 (2010)
14. W. Brostow, et al., Materials Chemistry and Physics **124(1)**, 371-376 (2010)
15. F.J. DiSalvo, Science **285(5428)**, 703-706 (1999)
16. S.M. Manyakin, M.P. Volkov, A.A. Sidorov, Sbornik statej konferencii ICT (2005)
17. T.D. Alieva, N.M. Ahundova, D.Sh. Abdinov, Neorgan. Materialy **33(1)**, 27 (1997)
18. T.M. Azimov, K.E. Onarkulov, K.I. G'aynazarova, Austrian Journal of Technical and Natural Sciences (Scientific journal) **1-2**, 21-25 (2020)
19. B.I. Boltaks, *Diffuziya i tochechnye defekty v poluprovodnikah* («Nauka», L., 1972)
20. D.Sh. Gufrova, G.Sh. Ergasheva, T.M. Azimov, *Issledovanie diffuzionnyh processov, prohodnyh v prikontaktnoj oblasti termoelementa. Tehnicheskie i matematicheskie nauki* (Izd. «MCNO», Moskva, 2020)
21. S.M. Otajonov, R.N. Ergashev, Journal of Physics: Conference Series **2388(1)**, 012062 DOI: 10.1088/1742-6596/2388/1/012062
22. S.M. Otazhonov, R.N. Ergashev, Journal of Physics: Conference Series **2388(1)**, 012001 DOI: 10.1088/1742-6596/2388/1/012001